INTERNATIONAL JOURNAL FOR NUMERICAL METHODS IN FLUIDS
Int. J. Numer. Meth. Fluids **30**: 137–148 (1999)

THE VISCOUS OPTIMAL SHAPE DESIGN, VIA SPECTRAL SOLUTIONS

ADRIANA NASTASE*

Lehr und Forschungsgebiet Aerodynamik des Fluges, RWTH, Templergraben 55, 52062 Aachen, Germany

SUMMARY

The shape of a flying configuration is globally optimized if its camber, twist, thickness and the similarity parameters of its planform are determined in order to obtain a minimum drag at cruising Mach number. The optimum–optimorum (OO) theory of the author solves this problem by using a lower limit hyper-surface for the drag functional. A multipoint design is realized by using movable leading edge flaps. The iterative OO theory is used for the computation of the friction drag, for the determination of the viscosity effect in the optimal shape of the flying configuration and to perform the multidisciplinary design by including structure and thermal auxiliary conditions. A proposal of a fully-optimized shape of supersonic transport aircraft with twin integrated fuselages is also made. Copyright © 1999 John Wiley & Sons, Ltd.

KEY WORDS: aerodynamic optimal shape design; variational methods; supersonic flow; multipoint and multidisciplinary optimal design

1. THE OPTIMUM–OPTIMORUM THEORY AND THE INVISCID DESIGN

The inviscid optimal design uses an inviscid flow field as a starting solver for the optimization. The determination of the optimum–optimorum (OO) shape of the flying configurations (FC) leads to an extended variational problem with free-boundary for the inviscid drag functional:

$$C_{\mathrm{d}}^{(i)} \equiv \int_{S(x_1,x_2)} F[x_1, x_2, Z(x_1, x_2)]\, \mathrm{d}x_1\, \mathrm{d}x_2 = \min. \tag{1}$$

Here, the equations $Z(x_1, x_2)$ of the FCs surface and of the contour $S(x_1, x_2)$ of its planform are *a priori* unknown and are determined by solving this extended variational problem. According to the OO theory [1–6] the OO-FC is chosen among a set of admissible FC, which are defined by some common properties. Two FC belong to the same set if: their downwashes w and w^* (of the thin and thick symmetrical components of the FC respectively) are piecewise approximated through two superpositions of homogeneous polynoms of the same degree; their planforms are polygons that are related through affine transformations and the shapes of the FC fulfil the same auxiliary conditions. The free parameters of the optimization are the coefficients $\tilde{w}_{ij}$ and $\tilde{w}^*_{ij}$ of the polynomial expansions of w and w^* and the similarity parameters v_i of the FCs planforms. According to the authors numerical–analytical method [1–12], the lower limit hypersurface of the drag functional is defined, i.e.

* Correspondence to: Lehr und Forschungsgebiet Aerodynamik des Fluges, RWTH, Templergraben 55, 52062 Aachen, Germany.

CCC 0271–2091/99/100137–12$17.50

Figure 1. Inviscid OO shapes of the delta wing alone, Adela (c); of the integrated delta wing–fuselage configuration, Fadet (a); and of the integrated delta wing–fuselage–movable leading edge flaps configuration of variable geometry, Varidela, with retracted (a) and open (b) flaps.

$$(C_{\mathrm{d}}^{(i)})_{\mathrm{opt}} = f(v_i). \tag{2}$$

The location of the minimum of this hypersurface gives the best values of the similarity parameters v_i and the optimal corresponding FC is the OO-FC of the set. Well-suited geometrical and aerodynamical auxiliary conditions and the authors reinforced potential solutions, as in [1–12], are used as starting solutions for the optimal design of the inviscid OO shapes of the following three FC: the delta wing alone, Adela (Figure 1(c); Figure 3) (optimized at cruising Mach number $M_\infty = 2$, with 13 free parameters), as in [1–6], the integrated delta wing–fuselage configuration, Fadet (Figure 1(a)), as in [6–8] (with 26 free parameters) and the integrated delta wing–fuselage–movable leading edge flaps configuration of variable geometry, Varidela (Figure 1(a) and (b)) (with 39 free parameters), optimized at two different cruising Mach numbers M_∞^* and M_∞ as in [9–12]. This multipoint optimal design is realized by using open (Figure 1(b)) and retracted flaps (Figure 1(a)). The practical applications of these optimized shapes are: the unmanned FC for Adela, the optimal integrated supersonic transport aircraft (OI-STA) and the space vehicles (SV) in two stages (like Sänger) for Fadet and the one stage SV (like NASP) for Varidela. In Figure 2(b), a shape of an OI-STA is proposed.

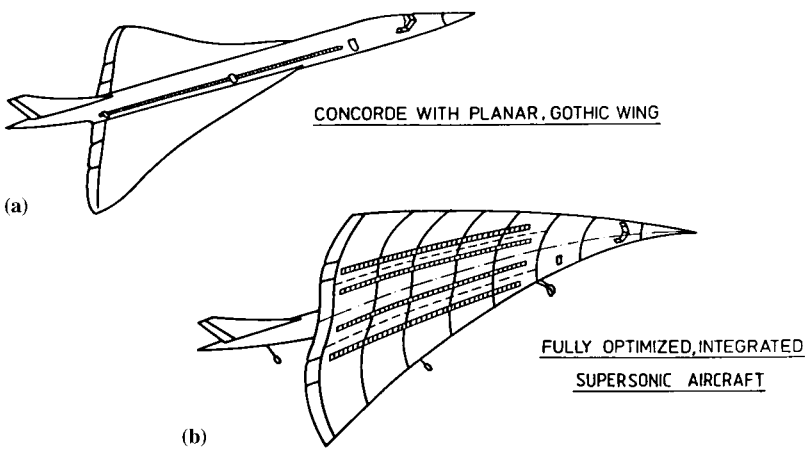

Figure 2. Proposed shape of an OI-STA (b) compared with that of Concorde (a).

2. THE INVISCID DESIGN OF THE OPTIMUM–OPTIMORUM SHAPE OF THE DELTA WING

The inviscid optimal design of the shape of the delta wing alone is further treated. Let us refer the thick, lifting delta wing with the similarity parameter of the planform $\nu = B\ell$ ($B = \sqrt{M_\infty^2 - 1}$ and $\ell = \ell_1 h_1$ with ℓ_1 the maximal half-span and h_1 the maximal depth) to a three-orthogonal system of co-ordinates $Ox_1x_2x_3$, having the vertex O at the apex of the wing. The Ox_1-axis has the direction tangent to the skeleton surface at the apex of the wing, in the symmetry plane Ox_1x_3 of the wing. The undisturbed velocity $\vec{V}_\infty$ is contained in this plane. This wing is flattened in the plane Ox_1x_2. The downwashes $\tilde{w}$ and $\tilde{w}^*$ are expressed in the form of superpositions of homogeneous polynoms in $\tilde{x}_1$ and $\tilde{x}_2$, i.e.

$$\tilde{w} = \sum_{m=1}^{N} \tilde{x}_1^{m-1} \sum_{k=0}^{m-1} \tilde{w}_{m-k-1,k} |\tilde{y}|^k, \qquad \tilde{w}^* = \sum_{m=1}^{N} \tilde{x}_1^{m-1} \sum_{k=0}^{m-1} \tilde{w}^*_{m-k-1,k} |\tilde{y}|^k. \tag{3a,b}$$

The axial disturbance velocities u and u^* for the delta wing components with subsonic leading edges are, as in [1–6], of the form:

$$u = \ell \sum_{n=1}^{N} \tilde{x}_1^{n-1} \left\{ \sum_{q=1}^{E((n-1)/2)} \tilde{C}_{n,2q} \tilde{y}^{2q} \cosh^{-1} \sqrt{\frac{1}{\tilde{y}^2}} + \sum_{q=0}^{E(n/2)} \frac{\tilde{A}_{n,2q} \tilde{y}^{2q}}{\sqrt{1-\tilde{y}^2}} \right\}, \tag{4}$$

$$u^* = \ell \sum_{n=1}^{N} \tilde{x}_1^{n-1} \left\{ \sum_{q=1}^{E((n-1)/2)} \tilde{C}^*_{n,2q} \tilde{y}^{2q} \cosh^{-1} \sqrt{\frac{1}{\nu^2 \tilde{y}^2}} + \sum_{q=0}^{n-1} \tilde{H}^*_{nq} \tilde{y}^q [\cosh^{-1} M_1 + (-1)^q \cosh^{-1} M_2] + \sum_{q=0}^{E((n-2)/2)} \tilde{D}^*_{n,2q} \tilde{y}^{2q} \sqrt{1-\nu^2\tilde{y}^2} \right\},$$

$$\left(M_{1,2} = \sqrt{\frac{(1+\nu)(1 \mp \nu\tilde{y})}{2\nu(1 \mp \tilde{y})}} \right). \tag{5}$$

Here is $\tilde{x}_1 = x_1/h_1$, $\tilde{x}_2 = x_2/\ell_1$, $\tilde{x}_3 = x_3/h_1$, $w = \tilde{w}$, $w^* = \tilde{w}^*$, $u = \ell\tilde{u}$, $u^* = \ell\tilde{u}^*$. The coefficients $\tilde{A}_{n,2q}$, $\tilde{C}_{n,2q}$ and $\tilde{H}^*_{nq}$, $\tilde{D}^*_{n,2q}$, $\tilde{C}^*_{n,2q}$ of $\tilde{u}$ and $\tilde{u}^*$ are related to the coefficients $\tilde{w}_{ij}$, $\tilde{w}^*_{ij}$ of $\tilde{w}$ and $\tilde{w}^*$ through linear and homogeneous relations, i.e.:

$$\tilde{A}_{n,2q} = \sum_{j=0}^{n-1} \tilde{a}^{(n)}_{2q,j} \tilde{w}_{n-j-1,j}, \qquad \tilde{H}^*_{nq} = \sum_{j=0}^{n-1} \tilde{h}^{*(n)}_{qj} \tilde{w}^*_{n-j-1,j}, \text{ etc.} \tag{6a,b}$$

The coefficients $\tilde{a}^{(n)}_{2q,j}$, $\tilde{c}^{(n)}_{2q,j}$, $\tilde{h}^{*(n)}_{qj}$, $\tilde{d}^{*(n)}_{2q,j}$, $\tilde{c}^{*(n)}_{2q,j}$ are non-linear functions only of ν. Let us first perform the optimal inviscid design of the thin delta wing, as in [1–6]. The optimal values of the coefficients $\tilde{w}_{ij}$, for a given value of ν, are obtained by setting the drag functional

$$C_d \equiv \ell \sum_{n=1}^{N} \sum_{m=1}^{N} \sum_{k=0}^{m-1} \sum_{j=0}^{n-1} \tilde{\Omega}_{nmkj} \tilde{w}_{m-k-1,k} \tilde{w}_{n-j-1,j} = \min, \tag{7}$$

with the following auxiliary conditions: the lift coefficient C_ℓ is given and the Kutta condition on subsonic leading edge (i.e. $u_{\tilde{y}\to 1} = 0$) is fulfilled in order to suppress the induced drag at cruising Mach number M_∞, i.e.

$$\tilde{C}_\ell \equiv \sum_{n=1}^{N} \sum_{j=0}^{n-1} \tilde{\Lambda}_{nj} \tilde{w}_{n-j-1,j} = \frac{C_{\ell_0}}{\ell}, \qquad \tilde{F}_n \equiv \sum_{j=0}^{n-1} \tilde{\Psi}_{nj} \tilde{w}_{n-j-1,j} = 0, \tag{8a,b}$$

with $n = 0, 1, \ldots, (N-1)$. The coefficients $\tilde{w}_{ij}$ and the Lagrange multipliers $\lambda^{(1)}$ and λ_n, as in [1–6], are given by solving of the following algebraic system formed by Equations (8a,b) and the equations obtained by the cancellation of the coefficients of each variation $\delta\tilde{w}_{\theta\sigma}$, i.e.:

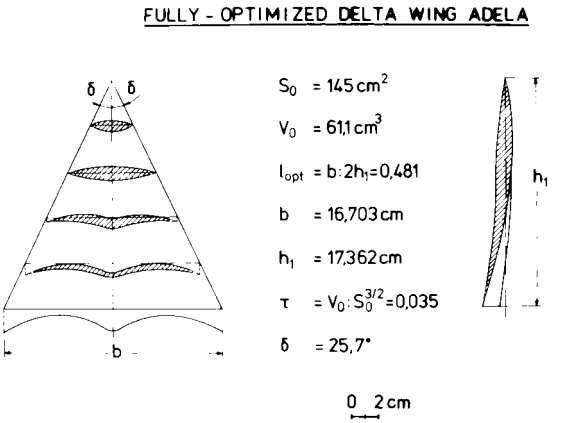

Figure 3. The OO-shape of the delta wing model Adela designed by the author with her own rapid software.

$$\sum_{n=1}^{N}\sum_{j=0}^{n-1}[\tilde{\Omega}_{n,\theta+\sigma+1,\sigma,j}+\tilde{\Omega}_{\theta+\sigma+1,n,j,\sigma}]\tilde{w}_{n-j-1,j}+\lambda^{(1)}\tilde{\Lambda}_{\theta+\sigma+1,\sigma}+\lambda_{\theta+\sigma+1}\tilde{\Psi}_{\theta+\sigma+1,\sigma}=0, \tag{9}$$

with $1<\theta+\sigma+1<N$, $\theta=0,1,\ldots,(N-1)$. Now, if the optimal design of the thick symmetrical delta wing is considered, the optimal values of the coefficients $\tilde{w}_{ij}^{*}$, for a given v, are obtained by setting the corresponding drag functional

$$C_{\mathrm{d}}^{*}\equiv\ell\sum_{n=1}^{N}\sum_{m=1}^{N}\sum_{k=0}^{m-1}\sum_{j=0}^{n-1}\tilde{\Omega}_{nmkj}^{*}\tilde{w}_{m-k-1,k}^{*}\tilde{w}_{n-j-1,j}^{*}=\min, \tag{10}$$

with the following auxiliary conditions: the relative volume ($\tau_0^{*}=V_0/S_0^{3/2}$) is given and the thickness cancels along the leading edge, i.e.

$$\tilde{\tau}^{*}\equiv\sum_{m=1}^{N}\sum_{k=0}^{m-1}\tilde{\tau}_{mk}^{*}\tilde{w}_{m-k-1,k}^{*}=\tau_0^{*}\sqrt{\ell},\qquad \tilde{E}_t^{*}\equiv\sum_{m=t+1}^{N}\sum_{k=0}^{m-1}\tilde{d}_{mk}^{*(t)}\tilde{w}_{m-k-1,k}^{*}=0, \tag{11a,b}$$

with $t=0,1,\ldots,(N-1)$. The coefficients $\tilde{w}_{ij}^{*}$ and the Lagrange multipliers $\mu^{(1)}$ and μ_t are given by the solving of the following algebraic system, as in [1–6]:

$$\sum_{n=1}^{N}\sum_{j=0}^{n-1}[\tilde{\Omega}_{n,\theta+\sigma+1,\sigma,j}^{*}+\tilde{\Omega}_{\theta+\sigma+1,n,j,\sigma}^{*}]\tilde{w}_{n-j-1,j}^{*}+\mu^{(1)}\tilde{\tau}_{\theta+\sigma+1,\sigma}^{*}+\sum_{t=0}^{N-1}\mu_t\tilde{d}_{\theta+\sigma+1,\sigma}^{*(t)}=0, \tag{12}$$

with $1<\theta+\sigma+1<N$, $\theta=0,1,\ldots,(N-1)$.

Now, if the optimization problem of the shape of the thick, lifting delta wing is treated, Equations (9) and (8a,b) and (12) and (11a,b) are coupled through the parameter v. The hybrid numerical–analytical method allows, as in [1–6], the numerical decoupling of these equations, which are strongly non-linear in v. Instead, to solve a non-linear system, a cascade of linear systems, obtained by giving several discrete values to v ($0<v<1$), is solved. The lower limit curve of the inviscid drag $(C_{\mathrm{d}}^{(i)})_{\mathrm{opt}}=f(v)$ is obtained. Each point of this curve is analytically obtained by solving of a variational problem with given boundary (i.e. given v). The location of the minimum of this curve is numerically determined and is the optimal value of v ($v=v_{\mathrm{opt}}$). If v_{opt} is introduced into (9) and (12), the best values of $\tilde{w}_{ij}$ and $\tilde{w}_{ij}^{*}$ are obtained respectively. According to the OO theory, rapid optimization software were developed by the author and used for the design of the OO Adela (Figure 3), for $M_\infty=2$, $\tau=0.035$, $C_\ell=0.12$ at $\alpha=0°$)

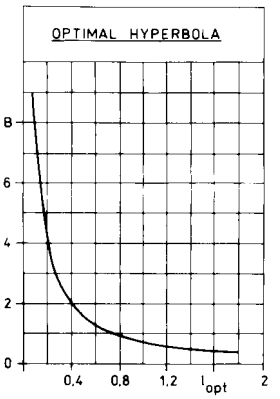

Figure 4. The optimal hyperbola used to find the optimal dimensionless span ℓ_{opt}, as a function of the cruising number $M_\infty = \sqrt{1 + B^2}$.

and for a systematical analysis of the influence of the initial parameters of the optimization (M_∞, C_ℓ and τ) over the shape of 100 optimized delta wings. This analysis leads to the conclusion that the correct choice of the optimal dimensionless span ℓ_{opt} by using the optimal hyperbola, as in Figure 4, and of the optimal angle of aperture γ_{opt} in functions of M_∞ and τ, as in Figure 5(a) and (b), causes an important drag reduction of the delta wing's shape.

3. EXPERIMENTAL RESULTS ON OPTIMUM–OPTIMORUM DELTA WING ADELA

In the frame of DFG research contracts of our Lehrgebiet, measurements of pressure, lift, pitching moment coefficients C_{p}, C_ℓ and C_{m} for the range of Mach numbers $M_\infty = (1.25 \sim 4)$

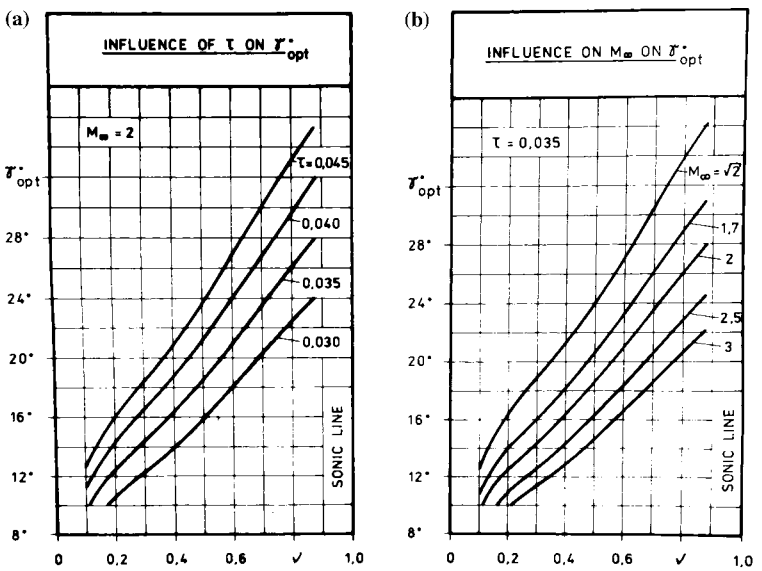

Figure 5. The optimal angle of aperture γ_{opt} in functions of M_∞ and τ.

Figure 6. Various delta and rectangular wing models.

and angles of attack $\alpha = (-20° \sim 20°)$ were performed in the trisonic wind tunnel of DLR-Köln (with the test section 60×60 cm^2) on four delta and two rectangular wing models (i.e. the wedged, the double wedged and the OO Adela delta wings, the wedged delta wing fitted with the conical fuselage, the wedged and the cambered rectangular wings) as given in the Figure 6. This was performed in order to explore the supersonic flow over the FC, to check the domain of validity for some reinforced (i.e. matched with the boundary layer) potential solutions of the author for the three-dimensional hyperbolical boundary value problems for u and u^* on the FC in supersonic flow, to check her software for the computation of C_p, C_ℓ and C_m of the FC, and to determine the optimal cruising Mach number of the OI-STA! In Figure

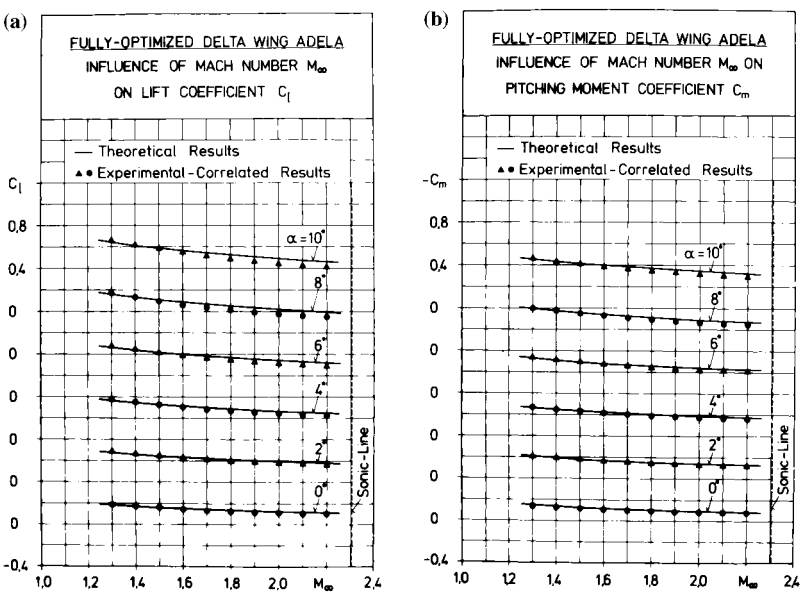

Figure 7. Comparisons of the theoretically with the experimentally determined aerodynamic characteristics C_ℓ and C_m of the OO model Adela (Figure 3) versus the Mach number M_∞ for the range of angles of attack $\alpha = (0° \sim 10°)$, showing good agreement for the range of $M_\infty = (1.25 \sim 2.2)$ considered in this study.

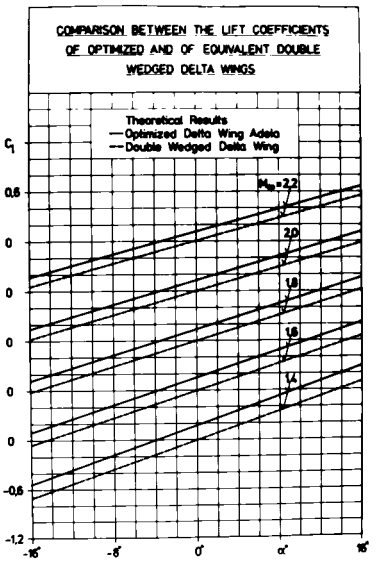

Figure 8. A comparison between the lift coefficients of the OO Adela and of an equivalent double-wedged delta wing with the same planform, volume and position of the maximal relative thickness as the OO Adela, shows that the Kutta condition along the leading edges leads to an important gain in lift.

7(a) and (b), the comparison of the theoretically with the experimentally determined aerodynamic characteristics C_ℓ and C_m of the OO model Adela (Figure 3) versus the Mach number M_∞ for the range of angles of attack $\alpha = (0° \sim 10°)$, shows good agreement, for the range of $M_\infty = (1.25 \sim 2.2)$ considered here. In Figure 8, a comparison between the lift coefficients of the OO Adela and of an equivalent double-wedged delta wing (with the same planform, volume and position of the maximal relative thickness as the OO Adela) shows that the Kutta condition along the leading edges leads to an important gain in lift. In Figure 9(a)–(c), the comparison of the theoretically with the experimentally determined C_p values, on the upper side of Adela, in the transversal section $\tilde{x}_1 = 0.599$ at the angles of attack $\alpha = (-8°, 0°, 8°)$ for the Mach numbers $M_\infty = (1.25, 1.4, 1.8, 2.2)$ shows good agreement. The experimental results confirm the theoretical predicted values of C_p, C_ℓ and C_m of the author, for large ranges of angles of attack and Mach numbers. The theoretical values of C_p for the thin and the thick symmetrical delta wings, are used as starting solutions and C_ℓ enters in the auxiliary conditions of the inviscid optimization of the thick, lifting delta wing taken alone.

4. THE ITERATIVE OPTIMUM–OPTIMORUM THEORY AND THE MULTIDISCIPLINARY VISCOUS DESIGN

An iterative OO theory is proposed here, as in Figure 10, in order to compute the friction drag and to determine the contribution of the viscosity in the optimal shape of the FC. The inviscid OO shape of the FC now represents the first step in an iterative shape optimization process. An intermediate computational checking of the inviscid OO shape is made with a spectral, zonal potential/three-dimensional boundary layer viscous solver of the author, as in [15–18]. The shear stress and the skin friction drag coefficient τ_w, $C_d^{(f)}$ of the FC are determined. The viscosity coefficient μ_w depends only on the temperature T.

The inviscid OO shape is checked also from the thermal and structural point of view. Additional auxiliary conditions introduced for thermal, structural or boundary layer reasons can occur. In the second step of optimization, the predicted inviscid optimized shape of the configuration is corrected by including these supplementary auxiliary conditions in the variational problem, and the friction coefficient in the drag functional. The iterative optimization process is repeated until the maximal local modification of the shape in two consecutive optimization steps presents no significant change. The proposed scheme allows the performing

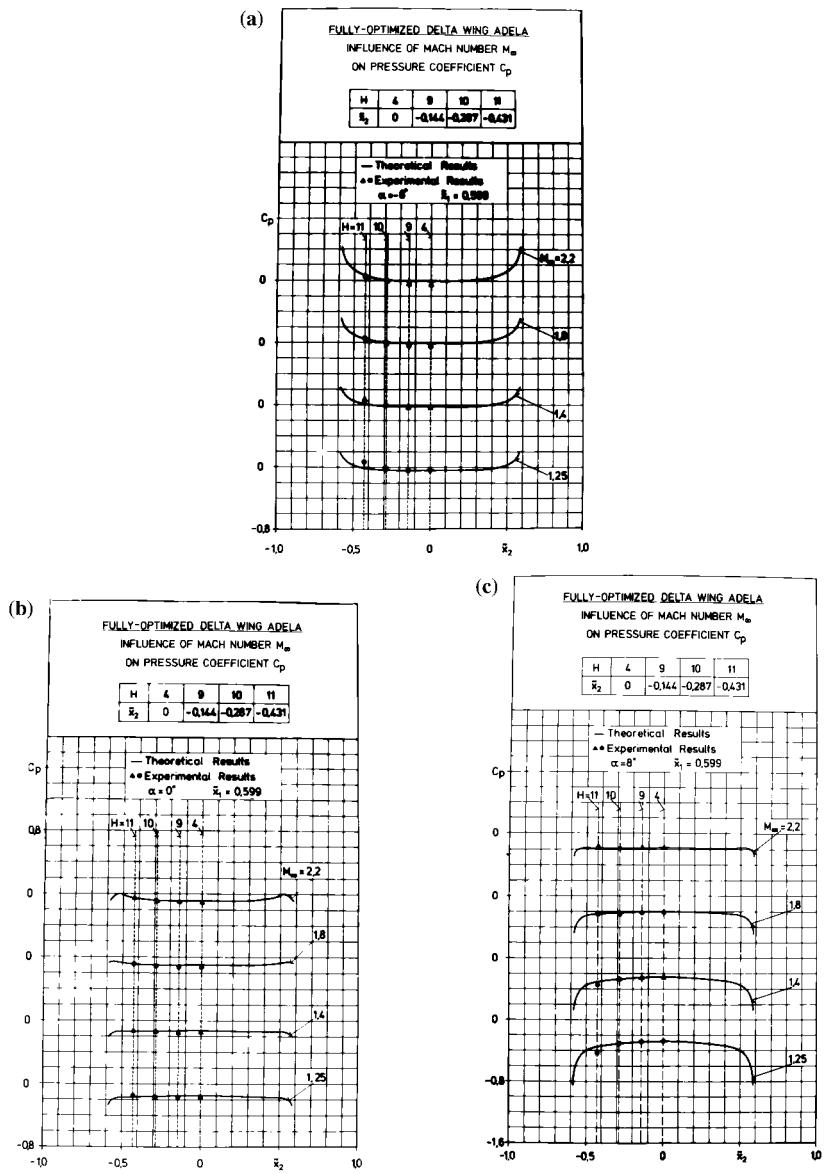

Figure 9. Comparisons of the theoretically with the experimentally determined C_p values, on the upper side of Adela, in the transversal section $\tilde{x}_1 = 0.599$ at the angles of attack $\alpha = (-8°, 0°, 8°)$ for the Mach numbers $M_\infty = (1.25, 1.4, 1.8, 2.2)$, showing good agreement.

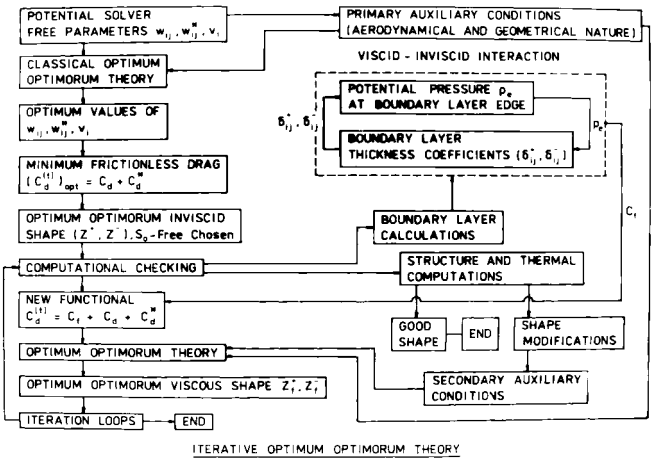

Figure 10. A proposed iterative OO theory.

of the multidisciplinary aerodynamical/structural optimal design. A weak coupling is realized via auxiliary conditions. Further, the author's spectral solutions are presented here. Let $\tilde{\delta}^+$ and $\tilde{\delta}^-$ denote the dimensionless thicknesses of the boundary layers on the upper and lower sides of the delta wing respectively. The slopes of the boundary layer thicknesses $\tilde{\delta}^+$ and $\tilde{\delta}^-$ in the Ox_1-direction are expressed in a form of superposition of homogeneous polynoms, as in [15–18], i.e.

$$\frac{\partial \tilde{\delta}^+}{\partial \tilde{x}_1} = \sum_{m=1}^{N} \tilde{x}_1^{m-1} \sum_{k=0}^{m-1} \tilde{\delta}^+_{m-k-1,k} |\tilde{y}|^k, \qquad \frac{\partial \tilde{\delta}^-}{\partial \tilde{x}_1} = \sum_{m=1}^{N} \tilde{x}_1^{m-1} \sum_{k=0}^{m-1} \tilde{\delta}^-_{m-k-1,k} |\tilde{y}|^k. \tag{13a,b}$$

The modified downwashes $\tilde{w}_1$ and $\tilde{w}_1^*$, due to the solidification of the boundary layer, are of the following form:

$$\tilde{w}_1 = \sum_{m=1}^{N} \tilde{x}_1^{m-1} \sum_{k=0}^{m-1} \tilde{w}^{(1)}_{m-k-1,k} |\tilde{y}|^k, \qquad \tilde{w}_1^* = \sum_{m=1}^{N} \tilde{x}_1^{m-1} \sum_{k=0}^{m-1} w^{*(1)}_{m-k-1,k} |\tilde{y}|^k. \tag{14a,b}$$

The modified coefficients in these formulas of $\tilde{w}_1$ and $\tilde{w}_1^*$ are

$$\tilde{w}^{(1)}_{ij} = \tilde{w}_{ij} + \frac{1}{2}(\tilde{\delta}^+_{ij} - \tilde{\delta}^-_{ij}), \qquad \tilde{w}^{*(1)}_{ij} = \tilde{w}^*_{ij} + \frac{1}{2}(\tilde{\delta}^+_{ij} - \tilde{\delta}^-_{ij}). \tag{15a,b}$$

The modified axial disturbance velocities u_1 and u_1^* at the edge of the boundary layer, in the second iteration, are obtained by replacing in (3a,b)–(6a,b), the inviscid coefficients $\tilde{w}_{ij}$, $\tilde{w}^*_{ij}$ with the modified ones $\tilde{w}^{(1)}_{ij}$, $\tilde{w}^{*(1)}_{ij}$. Further, the axial, lateral and vertical velocities u, v and w respectively, in the boundary layer are written in spectral forms, i.e.

$$u = u_e \sum_{i=1}^{N} u_i \eta^i, \qquad v = v_e \sum_{i=1}^{N} v_i \eta^i, \qquad w = w_e \sum_{i=1}^{N} w_i \eta^i. \tag{16a–c}$$

Hereby, u_e, v_e and w_e are the inviscid axial, lateral and vertical velocities at the edge of the boundary layer and $\eta = [x_3 - Z(\tilde{x}_1, x_2)]/\delta(\tilde{x}_1, x_2)$. The non-slip conditions on the wing's surface (i.e. $u = v = w = 0$ for $\eta = 0$) are automatically satisfied. The matching conditions with the potential flow, at the edge of the boundary layer (i.e. for $\eta = 1$) are $u = u_e$, $u' = u'' = 0$; $v = v_e$, $v' = v'' = 0$, $w = w_e$ and the continuity equation, written in P points Q_p $(p = 1, 2, \ldots, P)$ lead to the linear relations among the coefficients u_i, v_i, w_i, i.e.

$$\sum_{i=1}^{N} u_i = 1, \qquad \sum_{i=1}^{N} iu_i = 0, \qquad \sum_{i=1}^{N} i(i-1)u_i = 0;$$

$$\sum_{i=1}^{N} v_i = 1, \qquad \sum_{i=1}^{N} iv_i = 0, \qquad \sum_{i=1}^{N} i(i-1)v_i = 0;$$

$$\sum_{i=1}^{N} w_i = 1, \qquad \sum_{i=1}^{N} (D_{ip}u_i + E_{ip}v_i + F_{ip}w_i) = 0. \tag{17a–h}$$

Here $P = 3N - 3K - 7$ for the three-dimensional and $P = 2N - 2K - 4$ for the two-dimensional flow. The continuity, the impulse, the physical gas and the energy equations are used as in [13,14]. Further, in the boundary layer $p = p_e(\tilde{x}_1, \tilde{x}_2)$. The physical gas equation and an exponential law for the dependence of the viscosity μ on the absolute temperature T are used to eliminate T and μ from the impulse equations. These equations, written in K chosen points Q_k $(k = 1, 2, \ldots, K)$ in the boundary layer are:

$$\sum_{i=1}^{N}\sum_{j=1}^{N} u_i(A_{ijk}^{(1)}u_j + B_{ijk}^{(1)}v_j + C_{ijk}^{(1)}w_j) = D_k^{(1)} + \sum_{i=1}^{N} (A_{ik}^{(1)}u_i + B_{ik}^{(1)}v_i + C_{ik}^{(1)}w_i),$$

$$\sum_{i=1}^{N}\sum_{j=1}^{N} v_i(A_{ijk}^{(2)}u_j + B_{ijk}^{(2)}v_j + C_{ijk}^{(2)}w_j) = D_k^{(2)} + \sum_{i=1}^{N} (A_{ik}^{(2)}u_i + B_{ik}^{(2)}v_i + C_{ik}^{(2)}w_i),$$

$$\sum_{i=1}^{N}\sum_{j=1}^{N} w_i(A_{ijk}^{(3)}u_j + B_{ijk}^{(3)}v_j + C_{ijk}^{(3)}w_j) = \sum_{i=1}^{N} C_{ik}^{(3)}w_i. \tag{18a–c}$$

Equations (17a–h) are linear in u_i, v_i and w_i, and can be explicitly written with respect to $P + 7$ chosen variables u_i, v_i and w_i for the three-dimensional (and $P + 4$ variables for the two-dimensional) flow. These chosen variables are further introduced in (18a–c) and eliminated from these equations. A quadratic algebraic system of $M = 3K$ equations, for $3K$ remaining variables u_i, v_i, w_i for the three-dimensional flow (and $M = 2K$ equations for $2K$ remaining variables u_i and w_i for the two-dimensional flow), is obtained:

$$\sum_{i=1}^{M} a_{ii}^{(k)} X_i^2 = R_k. \tag{19}$$

Here is $M = 3K$ for the three-dimensional ($M = 2K$ for the two-dimensional) flow and

$$X_i = \begin{cases} u_i \\ v_i, \\ w_i \end{cases} \qquad a_{ijk}^{(1)} = \begin{cases} A_{ijk}^{(1)} \\ B_{ijk}^{(1)}, \\ C_{ijk}^{(1)} \end{cases} \qquad a_{ijk}^{(2)} = \begin{cases} A_{ijk}^{(2)} \\ B_{ijk}^{(2)}, \\ C_{ijk}^{(2)} \end{cases} \qquad a_{ijk}^{(3)} = \begin{cases} A_{ijk}^{(3)} \\ B_{ijk}^{(3)}, \\ C_{ijk}^{(3)} \end{cases}$$

$$a_{ij}^{(k)} = \begin{cases} a_{ijk}^{(1)} & i < i < M \\ a_{ijk}^{(2)} & M + 1 < i < 2M \\ a_{ijk}^{(3)} & 2M + 1 < i < 3M \end{cases}.$$

Further, if the notation $x_i = X_i^2$ is made, the solving of the QAS (19) is obtained by the iterative solving of a cascade of linear algebraic systems. In order to increase the rapidity of convergence and to obtain all the solutions of the QAS, the software must be written in complex. The coefficients $a_{ii}^{(k)}$ in the system (19) depend on the positions of the points P_k and on δ. The coefficients R_k, depend additionally, on ϱ. If δ and ϱ are initially guessed in the boundary layer, the $3M$ coefficients u_i, v_i and w_i are obtained by solving the system (19) and the additional $3(N - M)$ coefficients u_i, v_i and w_i are obtained for the linear equations (17a–h),

written in explicit form. The continuity equation and the physical equation of gas are used to correct ϱ and δ in the higher-order iteration loops. The shear stress τ_w at the wall and the global friction drag coefficient $C_d^{(f)}$, of the delta wing are

$$\tau_w = \mu \left.\frac{\partial u_\delta}{\partial \eta}\right|_{\eta=0} = \mu u_1 u_e, \qquad C_d^{(f)} = 8 v_f u_2 \int_{\tilde{O}\tilde{A}_1\tilde{C}} u_e \tilde{x}_1 \, d\tilde{x}_1 \, d\tilde{y}. \tag{20a,b}$$

The viscous optimized shape of the delta wing obtained after the performing of the third iteration of the optimal design presents no significant change, except on its rear part, which is thicker and more cambered than the inviscid one. The iterative OO theory is able to compute the total drag $C_d^{(t)} = C_d^{(f)} + C_d + C_d^*$, which is 30% greater than the inviscid drag (at $M_\infty = 2$, $\alpha = 0°$).

5. PROPOSAL OF A FULLY INTEGRATED SUPERSONIC TRANSPORT AIRCRAFT

The viscous optimal design shows that the contribution of the viscosity in the total drag is important, but the shape's modification, due to the viscosity, is reduced. The author makes the hypothesis that the optimal shape of the FC is that which restores the conditions of the potential flow around the FC, i.e. the flight of FC is with characteristics instead of shocks and the leading edge vortices are avoided for a large range of Mach numbers and angles of attack.

The exploration of supersonic flow with six models for the ranges of Mach number $M_\infty = (1.25 \sim 4)$ and angles of attack $\alpha = (-20° \sim 20°)$ leads to the conclusions that there exists a range of Mach numbers between $M_\infty = (1.6 \sim 2.8)$ in which it is possible to fly economically and ecologically with characteristics instead of shocks, if the aircraft configuration is sufficiently flattened and has a smooth surface!

A fully optimized, total integrated shape of the supersonic transport aircraft (OI-STA) designed for the cruising Mach number $M_\infty = 2$ is proposed here (Figure 2(b)) and compared with Concorde (Figure 2(a)). The OI-STA presented here is better integrated and more flattened because, instead of one great cylindrical fuselage, a total integrated twin configuration (i.e. two smaller cylindrical fuselages integrated inside the structure and joined with a stiffened structure) is used. This OI-STA presents the following advantages:

- due to the optimization with respect of minimum drag this configuration has a higher C_L/C_D;
- due to the Kutta condition along the leading edges, which leads to a suitable coupling of the camber and twist of the wing in each point, the cornet vortices on leading edges are cancelled. Therefore, the induced drag and the lateral instability are suppressed and the lift increases (see Figure 8) for a large range of Mach numbers and angles of attack;
- due to the integration, the OI-STA can be considered as one lifting wing and the shocks, the detachments and the vortices along the junction lines between the wing and the fuselage of the classical aircraft (with one cylindrical, non-integrated fuselage) are suppressed. It results in a reduced drag, and therefore, less fuel consumption and greater operating range;
- the multipoint optimal design is realized by using movable leading edges flaps that are optimized at a second lower Mach number M_∞^*. Additionally, for the start and landing blended trailing edge flaps, with the same outer shape as the shape of OI-STA (in the neighborhood of the trailing edges) are used, in order to avoid the increasing of drag at cruise;

– the multidisciplinary scheme proposed in Figure 10 allows an interactive structure and flight control of the optimal aerodynamic shape, via auxiliary conditions, which is possible in all the iteration loops of the iterative optimum–optimorum theory.

REFERENCES

1. A. Nastase, *Forme Aerodinamice Optime prin Metoda Variationala (Optimal Aerodynamic Shapes by Means of Variational Methods)*, Academy, Romana, 1969.
2. A. Nastase, *Utilizarea Calculatoarelor in Optimizarea Formelor Aerodinamice (Use of Computers for the Optimization of Aerodynamic Shapes)*, Academy, Romana, 1973.
3. A. Nastase, 'Eine graphisch-analytische Methode zur Bestimmung der Optimum–Optimorum Form des dünnen Deltaflügels in Überschallströmung', *RRST-SMA*, **1**, 19 (1974).
4. A. Nastase, 'Eine graphisch-analytische Methode zur Bestimmung der Optimum–Optimorum Form des symmetrisch-dicken Deltaflügels in Überschallströmung', *RRST-SMA*, **2**, 19 (1974).
5. A. Nastase, 'Die Theorie des Optimum–Optimorum Tragflügels im Überschall', *ZAMM*, **57** (1977).
6. A. Nastase, *Wing Optimization and Fuselage Integration for Future Generation of Supersonic Aircraft*, Israel Journal of Technology, Jerusalem, 1985.
7. A. Nastase, 'Computation of fully optimized wing–fuselage configuration for future generation of supersonic aircraft', in F. Payne, C. Corduneanu, A.H. Sheikh and T. Huang (eds.), *Proc. of IMSE 86*, Hemisphere, Washington DC, 1986.
8. A. Nastase, 'Optimum–optimorum integrated wing–fuselage configuration for supersonic transport aircraft of second generation', *Proc. of 15th ICAS Congress*, London, UK, 1986.
9. A. Nastase, 'The design of optimum–optimorum shape of space vehicle', in E. Higbea and J.A. Vedda (eds.), *Proc. 1st Int. Conf. on Hypersonic Flight in the 21st Century*, University of North Dakota, Grand Forks, 1988.
10. A. Nastase, 'The design of supersonic aircraft and space vehicles by using global optimization techniques', *Collection of Technical Papers ISCFD*, Nagoya, 1989.
11. A. Nastase, 'The optimum–optimorum shape of the space vehicle of variable geometry of minimum drag at two cruising Mach numbers', in A. Nastase (ed.), *Proc. of High Speed Aerodynamics 11*, 1990.
12. A. Nastase, 'The design of fully integrated shape of intercontinental supersonic transport aircraft of the second generation by using the global optimization techniques', *ICAS-Proc.*, Stockholm, 1990.
13. A.D. Young, *Boundary Layers*, Blackwell Scientific Publications, London, UK, 1989.
14. H. Schlichting, *Boundary Layer Theory*, McGraw-Hill, New York, 1979.
15. A. Nastase, 'The aerodynamic design via iterative optimum–optimorum theory', *Proc. IV Int. Symp. on Computational Fluid Dynamics*, vol. III, California Davis, CA, 1991.
16. A. Nastase, 'The design of fully optimized configurations by using the iterative optimum–optimorum theory', *ZAMM*, **72** (1992).
17. A. Nastase, 'The determination of hybrid analytical–numerical solutions for the three-dimensional compressible boundary layer equations', *ZAMM*, **73** (1993).
18. A. Nastase, 'Spectral solutions for the three-dimensional boundary layer and their application for the optimal viscous design', in H. Daiguji (ed.), *Proc. 5th Int. Symp. on Computational Fluid Dynamics*, Sendai, 1993.

